ISSN 1674-1056
http://cpb.iphy.ac.cn
http://iopscience.iop.org/cpb
中国物理 B
Chinese Physics
中国物理 Chinese Physics B

Acoustic characteristics of pulse detonation engine sound propagating in enclosed space

Yang Kang(康杨), Ning Li(李宁), Chun-Sheng Weng(翁春生), Xiao-Long Huang(黄孝龙)

Citation: Chin. Phys. B . 2020, 29(1): 014703 . **doi:** 10.1088/1674-1056/ab5b88
Journal homepage: http://cpb.iphy.ac.cn; http://iopscience.iop.org/cpb

What follows is a list of articles you may be interested in

Acoustic characteristics of pulse detonation engine with ellipsoidal reflector

Yang Kang(康杨), Ning Li(李宁), Chun-Sheng Weng(翁春生), Chuan-Wei Wang(王传位)

Chin. Phys. B . 2018, 27(10): 104703 . **doi:** 10.1088/1674-1056/27/10/104703

Three-dimensional detonation cellular structures in rectangular ducts using an improved CESE scheme

Yang Shen(沈洋), Hua Shen(申华), Kai-Xin Liu(刘凯欣), Pu Chen(陈璞), De-Liang Zhang(张德良)

Chin. Phys. B . 2016, 25(11): 114702 . **doi:** 10.1088/1674-1056/25/11/114702

Critical deflagration waves leading to detonation onset under different boundary conditions

Lin Wei, Zhou Jin, Fan Xiao-Hua, Lin Zhi-Yong

Chin. Phys. B . 2015, 24(1): 014701 . **doi:** 10.1088/1674-1056/24/1/014701

Particle path tracking method in two-and three-dimensional continuously rotating detonation engines

Zhou Rui, Wu Dan, Liu Yan, Wang Jian-Ping

Chin. Phys. B . 2014, 23(12): 124704 . **doi:** 10.1088/1674-1056/23/12/124704

Existence of a Hartmann layer in the peristalsis of Sisko fluid

Saleem Asghar, Tayyaba Minhas, Aamir Ali

Chin. Phys. B . 2014, 23(5): 054702 . **doi:** 10.1088/1674-1056/23/5/054702

Acoustic characteristics of pulse detonation engine sound propagating in enclosed space*

Yang Kang(康杨), Ning Li(李宁)†, Chun-Sheng Weng(翁春生), and Xiao-Long Huang(黄孝龙)

National Key Laboratory of Transient Physics, Nanjing University of Science and Technology, Nanjing 210094, *China*

(Received 12 August 2019; revised manuscript received 21 November 2019; accepted manuscript online 26 November 2019)

Acoustic characteristics of pulse detonation engine (PDE) sound propagating in enclosed space are numerically and experimentally investigated. The finite element software LS-DYNA is utilized to numerically simulate the PDE sound propagating in enclosed space. Acoustic measurement systems are established for testing the PDE sound in enclosed space, and the time-frequency characteristics of PDE sound in enclosed space are reported in detail. The experimental results show that the sound waveform of PDE sound in enclosed space are quite different from those in open space, and the reflection and superposition of PDE sound on the walls of enclosed space results in the sound pressure oscillating obviously. It is found that the peak sound pressure level (PSPL) and overall sound pressure level (OASPL) of PDE sound in enclosed space are higher than those in open space and their difference increases with the rise of propagation distance. The results of the duration of PDE sound indicate that the A duration of PDE sound in enclosed space is higher than that in open space except at measuring points located at 2-m and 5-m while the B duration is higher at each of all measuring points. Results show that the enclosed space has a great influence on the acoustic characteristic of PDE sound. This research is helpful in performing PDE experiments in enclosed laboratories to prevent the PDE sound from affecting the safety of laboratory environment, equipment, and staffs.

Keywords: pulse detonation engine, acoustics characteristics, enclosed space

PACS: 47.40.Rs, 43.25.Jh, 43.28.Mw **DOI:** 10.1088/1674-1056/ab5b88

1. 1. Introduction

The pulse detonation engine (PDE) has been recently recognized as an innovative propulsion technology that potentially provides significant advantages of high thermal cycle efficiency, mechanical simplicity, higher thrust-to-weight ratio, lower cost, and a wide working scope. Much progress has been made in many important performance aspects of PDE.[1] In order that the PDE can be successful commercially in serving as a propulsion system, the environmental influence of PDE should be considered as an important issue. In particular, most of the PDE experiments are now carried out in an enclosed space such as laboratory. The high power noise generated by PDE is harmful to the laboratory staff, experimental equipment and laboratory environment. However, relatively few work has been reported on PDE acoustics.

The preliminary studies provide an initial understanding of PDE acoustic behavior. Boesh *et al.*[2] measured the acoustic pressure downstream of a PDE along the tube axis direction. Results showed that the pressure time history and spectra of the exiting detonation waves were comparable to those obtained through ideal blast wave theory. Allgood *et al.*[3] investigated experimentally the acoustic behavior of PDE inside an anechoic chamber. Far-field acoustic directivity results were obtained, showing a strong variation of the overall sound pressure level (OASPL) with directivity angle. The upstream and sideline measurement angles showed a lower sound pressure level than the downstream angles. The effects of operating conditions including fill fraction, cycle frequency, and exhaust nozzle geometry on the acoustic behavior of PDE were also studied. The results showed an increase in OASPL with fill fraction and a logarithmic increase with PDE cycle frequency. The results also suggested that the acoustic levels were sensitive to both the nozzle length and area ratio. Shaw *et al.*[4] studied the acoustic environment of a PDE operating at 20 Hz or 40 Hz. The acoustic measurements were made near the exit of the tubes and extended up to a distance 12 feet away, and the results indicated that a very high level pulse was generated near the exit of the tubes but tended to decrease in amplitude fairly quickly with distance increasing since the higher frequency energy dissipates in the atmosphere. Radial decay data would be useful in evaluating the accuracy of PDE sound prediction schemes. Glaser *et al.*[5] explored the effect of the major operating parameters and exhaust exit geometries on the acoustic signature of PDE. The results showed that acoustic level increases with both fill fraction and equivalence ratio increasing and the OASPL increases logarithmically in the OASPL with operating frequency increasing. The acoustic signature of a PDE can be significantly changed by modifying the tube exit geometry. Attenuation levels of 6.5 dB were ob-

*Project supported by the National Natural Science Foundation of China (Grant Nos. 11372141 and 11472138), the Fundamental Research Funds for the Central Universities, China (Grant No. 30919011258), and the Young Scientists Fund of the Natural Science Foundation of Jiangsu Province, China (Grant No. BK20190439).

†Corresponding author. E-mail: phoenixkyo@163.com

© 2020 Chinese Physical Society and IOP Publishing Ltd

served under certain conditions. Further investigation results have been presented by Glaser *et al.*[6] The obtained results showed that the shock wave speed quickly decays from detonation speeds present near the tube exit to sonic speed at a short distance away from the exit. It was found that the PDE generated pressure field was reasonably modeled by a theoretical point-source explosion. Caldwell *et al.*[7] quantitatively evaluated the far-field acoustics of a dual-pulse detonation engine system and compared the far-field acoustics of a dual-pulse detonation engine system with that of a single-PDE system. The direct comparison showed that the addition of a second PDE firing at the same frequency as the frequency at whch a single PDE fires, results in an increase in the OASPL by about 3 dB. Zheng *et al.*[8] investigated the noise radiation characteristics of PDE and HPDE under several operating frequencies. The results showed that the sound pressure level of HPDE is about 4 dB less than that of PDE, and that the impulse sound pressure level reduces about 2 dB. Xu *et al.*[9–13] studied the formation and propagation process of PDE sound by combing the experimental method and numerical method. The results showed that the detonation peak noise is proportional to -3 power of the radial distance in near-field. The effects of different tubes and loading conditions on PDE sound were studied. The results showed that the convergent-divergent nozzle has the most significant influence on PDE sound to reduce the noise amplitude by 77.13% in 0° direction at 3000 mm. With increasing the fill fraction of PDE, the amplitude of shock noise and jet noise increase while the amplitude ratio of jet noise to shock noise decreases. Huang *et al.*[14–16] numerically and experimentally explored the mechanism of noise propagation out of PDE. The propagation region was divided into three subregions, which are strongly nonlinear subregion, weak nonlinear subregion and linear subregion. The calculated results showed that the largest rate of decay is 33 dB/m in the strongly nonlinear subregion while the least rate of decay is 1.02 dB/m in the weak nonlinear subregion. The noise characteristics of a dual-tube PDE system and three-tube system were experimentally investigated. The results showed that the directivity of dual-tube PDE sound is different at a different propagation distance. The highest PDE sound pressure appeared in 0° direction around PDE exit and it appeared in 30° direction in the region more than 2 m away from tube exit while the directivity of three-tube PDE kept unchanged in 30° at various radial distances. Kang *et al.*[17] investigated the acoustic characteristics of a PDE with and without an ellipsoidal reflector. The experimental results showed that the ellipsoidal reflector can realize the shock wave noise and jet noise focusing well, and create a focal zone on the PDE axis with very high pressure, and obviously slow down the pressure attenuation along the distance and over time in the downstream direction. The maximum relative increase ratio of PSPL and OASPL are obtained at focus point F_2 of the ellipsoidal reflector, whose values are 6.1% and 6.84% respectively. The greatest PSPL of PDE sound appears at a directivity angle of 20° while it changes to 0° directivity angle under the installation of the reflector.

In this study, experimental investigation is performed on a PDE in enclosed laboratory with long distance on a spatial scale. The acoustic characteristics of PDE sound including time-frequency characteristics, peak sound pressure level (PSPL), overall sound pressure level (OASPL) and duration are analyzed. It is found that the acoustic characteristics of PDE sound in enclosed space are quite different from those in open space.

2. Experimental system and computational analysis model

2.1. Experimental setup

In order to explore the detonation acoustic characteristic of PDE in enclosed space, the experimental system was set up as shown in Fig. 1. The experimental system was composed of a PDE tube, fuel and oxidizer supply apparatus, a control and ignition device and an acoustic measurement subsystem. The PDE tube is closed at one end and opened at the other, which is made of a 304 stainless steel pipe with an inner diameter of 80 mm. Two electromagnetic valves fed compressed oxygen and compressed air into the mixing chamber from tangential direction, and a separate valve supplies the liquid gasoline fuel into an atomizing spray nozzle which is installed at the head wall of the PDE tube. To enhance the atomization and vaporization of liquid fuel, a venturi tube was employed to accelerate the flow for secondary atomization of liquid fuel droplets. The mixtures were ignited by a spark plug which delivers energy, 1.5 J per spark, and the ignition frequency can be controlled easily by a signal from a generator. A Shchelkin spiral was inserted into the front of the detonation chamber to aid in the deflagration-to-detonation transition (DDT) process. In the present work, the equivalence ratio of the fuel and oxidizer mixture is maintained to be stoichiometric, $\phi = 1$. The fill fraction (ff), which was defined as the ratio of the volume of the detonation tube filled with a combustible mixture prior to ignition to the overall volume of the tube, is held constant at 1.0. The acoustic measurement system is specifically designed for obtaining acoustic data. Two PCB model 113B26 dynamic pressure sensors and four PCB model 377A12 microphones were adopted in the acoustic measurement system. The two dynamic pressure sensors were arranged at 2 m and 5 m from the PDE exit and the six microphones were arranged respectively at position 10 m, 20 m, 50 m, 80 m away. The heights of all sensors were consistent with the central axis of the detonation tube. The acoustic data of PDE were acquired at 500k samples/s for all sensors simultaneously by using a LabView interface program.

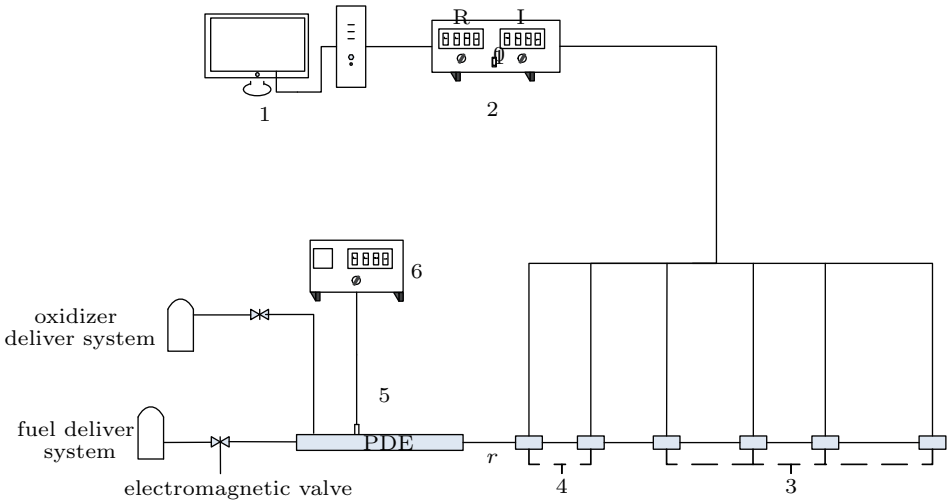


Fig. 1. Schematic diagram of experimental setup. 1: Data acquisition system, 2: A/D converter, 3: acoustic transducer, 4: pressure transducer, 5: spark plug, 6: ignition control system.

In order to compare the acoustic characteristics of PDE sound in enclosed space with that in open space, the same experimental system was also constructed in the open space.

The laboratory is a long, straight enclosed space with rough walls which are covered with sound-absorbing materials. Figure 2 indicates geometry parameters for the enclosed space used in this study. The rectangular enclosed space L was 187-m long and had a width W and height H of 4.5 m. The PDE exit was located at a position 3 m away from the left wall, and the central axis of the PDE tube is 1 m away from the bottom wall.

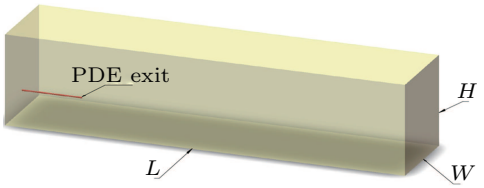


Fig. 2. Dimensions of enclosed space and PDE location.

2.2. Computational model

The physical process involved in the formation of gas–liquid two-phase detonation was especially complicated. This paper focuses on exploring the acoustic characteristics propagating of PDE sound in enclosed space. Therefore, the following assumptions were made in the establishment of the computational model. Firstly, the pressure waveform measured at the PDE exit was similar to the pressure waveform obtained by point explosion, which can be effectively loaded in the finite element software LS-DYNA. Then PDE sound source was equivalent to the point explosion source without considering the influence of the geometry or the size of PDE exit on the detonation wave propagation.

According to the explosion theory, the relationship between explosive charge mass M (in unit g) and shock wave energy E (in unit J) is expressed as

$$M = 0.24 \times 10^{-3} E. \tag{1}$$

The shock wave energy E is related to the volume of PDE V_{PDE}, the combustion enthalpy of the reactants detonated, and the operating fill-fraction ff by

$$E = V_{\mathrm{PDE}} \times H_{\mathrm{rec}} \times ff. \tag{2}$$

In the calculation, the fuel gasoline was replaced by n-octane, of which the combustion enthalpy was 44425 kJ/kg. The volume of PDE was 0.015 m^3, and the fill-fraction of fuel and oxidizer was 1. The calculation result of shock wave energy of PDE is 7740 kJ which converts into the mass of explosive charge, 1858 g. The explosive charge with density of 1.63×10^{-3} g/mm^3 was selected for computation, and the corresponding volume was 1.149×10^6 mm^3.

The arbitrary Lagrange–Euler (ALE) approach was used in the simulation and LS-DYNA used a coupled method for obtaining an optimal numerical results. In the numerical model, the explosive charge was typically modeled by using the Jones–Wilkins–Lee (JWL) equation of state (EOS), which modeled the pressure generated from the chemical energy in an explosion. It could be expressed as follows:

$$p(V,E) = A\left(1 - \frac{\omega}{R_1 V}\right)\mathrm{e}^{-R_1 V} + B\left(1 - \frac{\omega}{R_2 V}\right)\mathrm{e}^{-R_2 V} + \frac{\omega E}{V}, \tag{3}$$

where p is the hydrostatic pressure, V is the specific volume, E is the specific internal energy, and A, B, R_1, R_2, and ω are the material parameters. In this study, the parameters in Eq. (3) are given in Table 1.

Table 1. Parameters of explosive charge and JWL EOS (in cm-g-μs).

ρ_0	c_0	P_{CJ}	A	B	R_1	R_2	ω	E	V
1.63	0.693	0.21	3.712	0.032	4.5	0.95	0.3	0.07	1

Air was assumed to be an ideal gas that is able to satisfy the EOS. The pressure related to the energy could be expressed as follows:

$$p = (\gamma - 1)\rho e, \tag{4}$$

where γ is a constant, ρ is the air density, and e is the specific internal energy. In this study, the parameters in Eq. (4) are given in Table 2.

Table 2. Parameters in EOS of air (in cm-g-μs).

γ	ρ	e
1.4	1.29×10^{-3}	2.5×10^{-6}

The geometry of the computational domain was half the experimental space due to the symmetry of the enclosed space. The centroid of explosive charge was set to be at the position of PDE tube exit. The symmetrical boundary condition was set to be in the x–z plane, and the rigid boundaries were used for the walls for ignoring the absorption of explosion energy.

3. Computational analysis of PDE sound propagating in enclosed space

Figure 3 shows the pressure contours of shock wave propagating in the enclosed space.

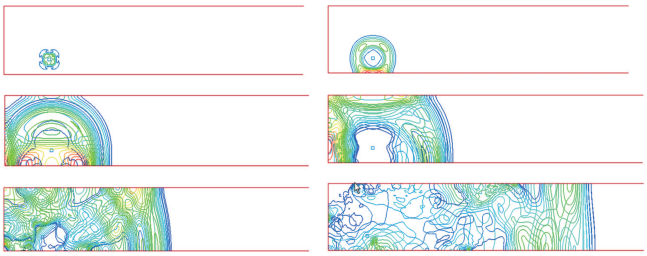


Fig. 3. Pressure contours of shock wave propagating in enclosed space.

In the near region away from the explosion source, the wave front extends outwards in different shapes. With the increase of time, the shock wave gradually changes into a spherical wave propagating along the axial direction and radial direction of the enclosed space. The first reflection occurs at the bottom wall because the distance from the center of the explosive charge to the bottom wall is the shortest. The shock wave is strengthened after reflecting by the wall and the propagation speed of the shock wave near the bottom wall is higher than that near the top wall. The reflected shock wave starts to catch up with the direct shock wave propagating to the top wall. The new reflection is produced when the shock wave arrives at the top wall. The reflected wave from the bottom wall is superposed with it, generating a new shock wave propagating to the bottom wall. When it arrives at the bottom wall, it will reflect again and multiple reflected wave effect will occur. The identical phenomenon occurs when the direct wave arrives at other walls. The direct wave and reflected wave also propagate along the axial direction of the enclosed space in the reflection and superposing process, and gradually attenuate with the increase of propagation distance, and finally form a stable plane wave to propagate forward.

4. Experimental analysis of PDE sound propagating in enclosed space

4.1. Time domain characteristics analysis of PDE sound in enclosed space

The PDE sound mainly comes from two sources, *i.e.*, the noise associated with the high-speed shock wave and the jet noise produced during the blowdown of the hot detonation products. When the detonation wave leaves the exit of the detonation tube, it quickly degenerates into a bow shock. With the propagation of the shock wave, it is attenuated into the shock noise. Subsequently, the high-pressure detonation products in the detonation wake expand rapidly out of the PDE tube in a spherical manner. The interaction between surrounding atmospheres forms a jet shock wave. The jet noise consists of the jet shock noise caused by the jet shock wave degradation and turbulent noise generated by the hot jet (see Fig. 4).

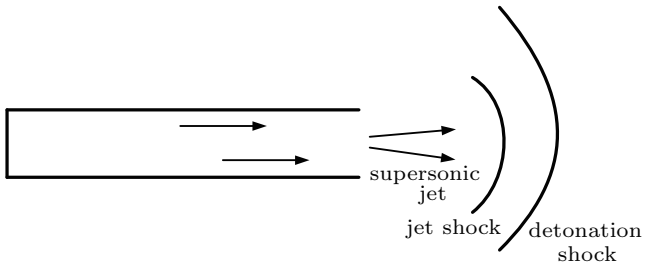


Fig. 4. Schematic diagram of PDE sound.[2]

The repeatability tests are performed and a typical far-field PDE sound waveform in enclosed space is selected for analyses. Figure 5(a) shows the experimental results of the sound pressure of PDE at the position 20 m away from the tube exit in the enclosed space at 5-Hz operation frequency and the single impulse sound waveform of PDE is shown in detail as shown in Fig. 5(b). It can be seen in Fig. 5(b) that, the first pressure peak p_1 and the second pressure peak p_2 represent the direct waves of the shock noise and the jet noise whose values are 1645.0 Pa and 2300.7 Pa respectively. A series of sound pressure peaks appear following the direct shock noise and the direct jet noise which are formed by the reflection and superposition of the shock noise and the jet noise restrained by the walls of the enclosed space.

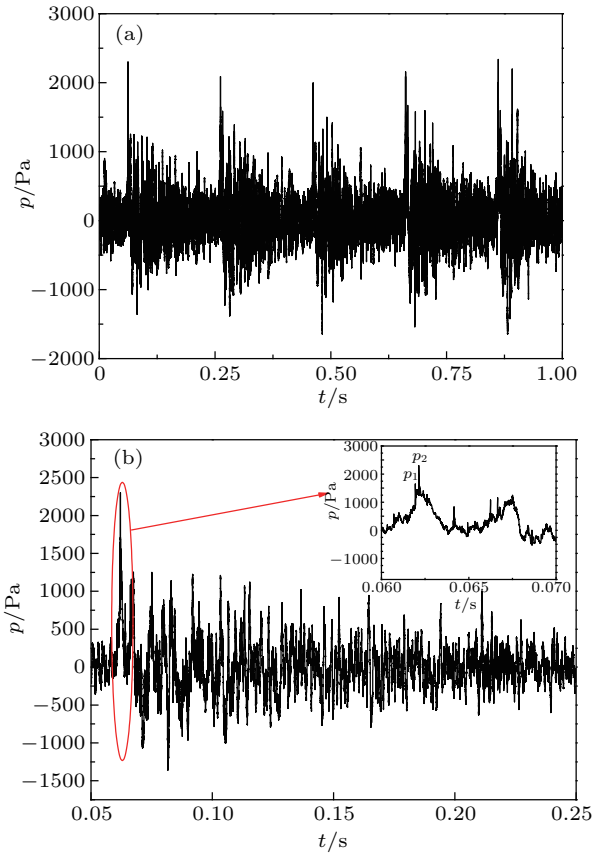


Fig. 5. (a) Sound waveform of PDE operating at 5 Hz in enclosed space. (b) Single impulse sound waveform of PDE in enclosed space.

Figure 6(a) shows the experimental sound pressure of PDE at the position 20 m away from the tube exit in open space at 5-Hz operation frequency. It can be easily found that the sound waveform of PDE sound in open space is significantly different from that in enclosed space. The PDE sound presents the characteristic of typical impulse noise. The definition of impulsive noise has been given in a China National Standard of GJB50-85, namely, the noise which is composed of one or more abrupt noises (its duration time is less than 1 s) can be called impulsive noise. The sound radiation characteristics of PDE sound are intermittent, periodically short in duration, and high in intensity. Figure 6(b) shows the single impulse sound waveform of PDE sound in open space in detail. The first positive pressure peak p_3 is for the shock noise formed by the detonation wave escaping from the nozzle. When the shock noise propagates to the test point, the sound pressure at the test point rises rapidly to 1133 Pa. The second positive pressure peak p_4 which represents jet noise comes 0.35 ms later and the value of p_4 is approximately 890.2 Pa. After the shock noise and jet noise pass through the test point, the sound pressure of PDE sound gradually decreases to atmospheric pressure, and a negative pressure phase appears on the waveform at a certain distance from the PDE exit. As shown in Fig. 6(b), a compensating negative pressure phase is fully developed, and the peak value of negative pressure is usually smaller than that of positive pressure. At the end of the negative pressure, the pressure basically recovered to the environmental pressure. No oscillation of the PDE sound pressure appears after the negative pressure phase.

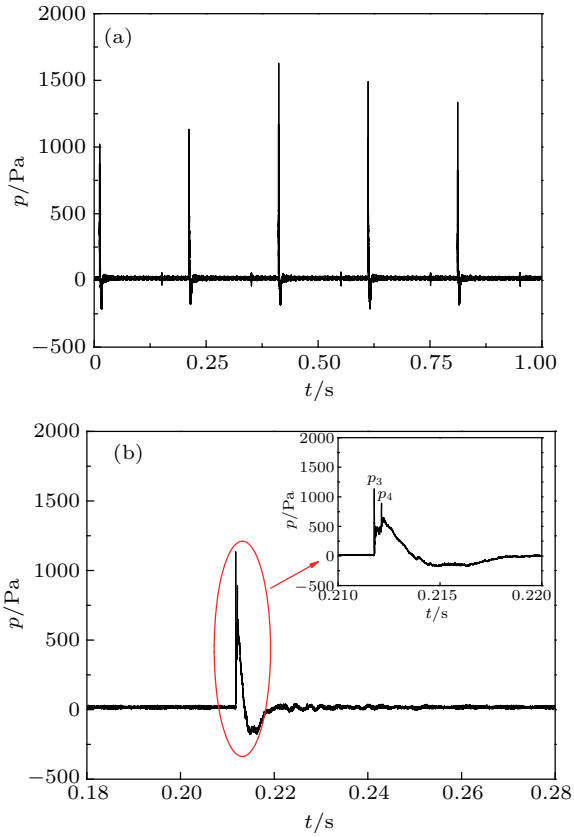


Fig. 6. PDE sound waveform at 20 m. (a) Sound waveform of PDE operating at 5 Hz in open space. (b) Single impulse sound waveform of PDE in open space.

To explore the PDE sound waveform at different propagation distances in enclosed space, PDE sounds respectively at the positions 2 m, 5 m, 10 m, 20 m, 50 m, 80 m away from the PDE exit which are marked from TP_{e1} to TP_{e6} in proper order are experimentally investigated. Figure 7 shows the experimental sound pressure of PDE sound at each measuring point in enclosed space. As shown in Figs. 7(a) and 7(b), a series of sound pressure peaks exists before the sound pressure reaches to the maximum pressure peak. The first pressure peak and the second pressure peak represent the direct waves of shock noise and jet noise respectively. Sound pressure peaks following the direct shock noise and direct jet noise are formed by the reflection and superposition of shock noise and jet noise, which are restrained by the walls of the enclosed space. With the constant dissipation of reflected sound energy, the value of peak sound pressure becomes smaller. The reflected noise in the enclosed space catches up with the direct noise with the increase of the propagation distance, and forms a stable PDE sound propagating forward in the enclosed space. As a result, the first sound pressure peak becomes the maximum sound pressure peak and the pressure oscillation after the peak pressure has become smooth at the measuring points after TP_{e2}.

Figures 7(a)–7(f) show obviously that the peak sound pressure of PDE sound decreases rapidly with the increasing propagation distance near the PDE exit. The peak sound pressure decreases from 54375.9 Pa at TP_{e1} to 10607.5 Pa at TP_{e2}, which decreases by about 80.5%. The peak sound pressures of PDE sound at other measuring points are 3390.7 Pa, 2300.8 Pa, 1263.1 Pa, and 1990.9 Pa, respectively. It can be concluded that the attenuation rate of the peak pressure of PDE sound becomes slower with the increase of propagation distance in enclosed space.

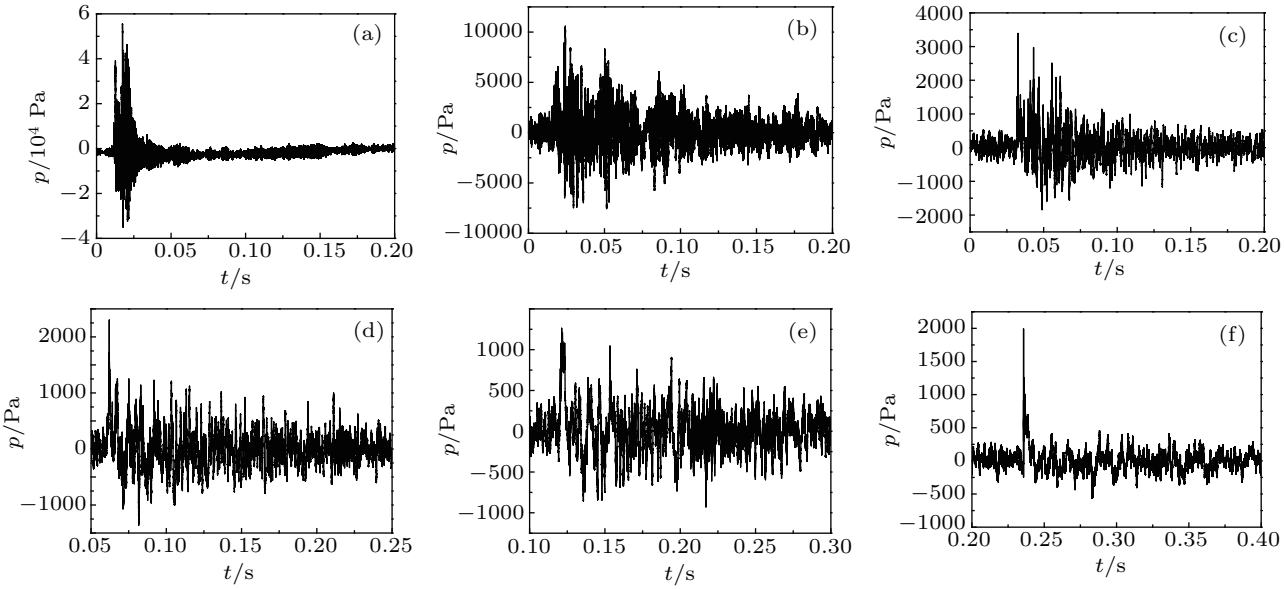


Fig. 7. PDE sound waveforms at different measuring points in enclosed space: (a) PDE sound waveforms at TP_{e1}, (b) PDE sound waveforms at TP_{e2}, (c) PDE sound waveforms at TP_{e3}, (d) PDE sound waveforms at TP_{e4}, (e) PDE sound waveforms at TP_{e5}, (f) PDE sound waveforms at TP_{e6}.

4.2. Frequency domain characteristics analysis of PDE sound in enclosed space

PDE sound is composed of sounds with different intensities and frequencies. The energy distribution in each frequency band of PDE sound is also different. The time domain signal of PDE sound at 20 m in the enclosed space is transformed by FFT method and the spectrum diagram is shown in Fig. 8(a). It can be easily found that PDE sound in enclosed space belongs to broadband noise, there are various frequency components between 0 and 100 kHz. The intensity of PDE sound changes in zigzag shape in the frequency band of 10 Hz–1000 Hz, and the sound pressure level fluctuates in a range of 108 dB–130 dB, which is mainly concentrated in a range of 125 dB–130 dB. It can be seen that the energy distribution of PDE sound is relatively uniform within a span of 1000 Hz. When the frequency of PDE sound exceeds 1000 Hz, the sound pressure level at the frequency point decreases with the increase of frequency and attenuation rate is −21.5 dB/decade.

Figures 8(b) shows the logarithmic acoustic spectra of PDE sound at 20 m in open space. The acoustic frequency spectrum is broad and ranges from 10 Hz to 100 kHz. In the frequency ranging from 10 Hz to 100 Hz, the intensity of the PDE sound first increases and then decreases with the increase of noise frequency. The peak sound pressure appears at the 120-Hz frequency of the PDE sound waveform, at which frequency the sound pressure level is 114.2 dB. In a frequency range from 1 kHz to 100 kHz, the intensity of the PDE sound changes in a zigzag manner. The sound pressure level generally decreases as the frequency of the PDE sound increases.

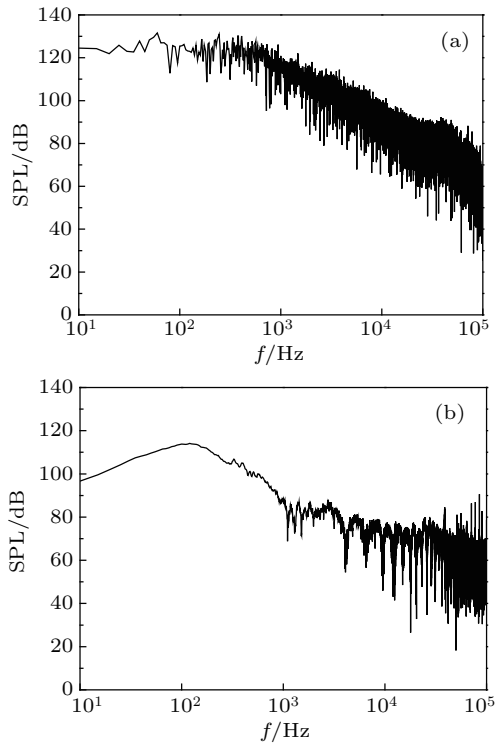


Fig. 8. Logarithmic acoustic spectrum of PDE sound at 20 m: (a) acoustic spectrum of PDE sound in enclosed space, (b) acoustic spectrum of PDE sound in open space.

The frequency domain characteristics of PDE sound at

each testing point are substantially identical except the peak frequency. Figure 9 shows the peak frequency of PDE sound in enclosed space varying with propagating distance. It can be easily found that with increasing propagation distance, the high frequency sound dissipates quickly and the peak frequency of PDE sound shifts toward lower frequencies. The analysis of the sound frequency spectrum shows the low frequency characteristic of PDE sound in enclosed space obviously.

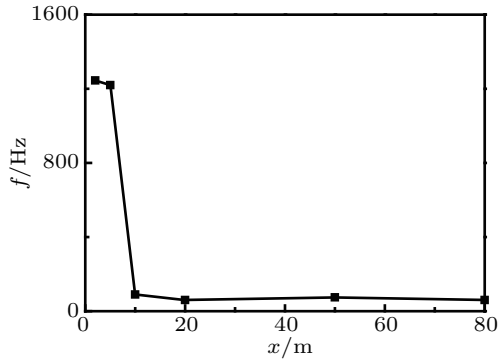


Fig. 9. Peak frequency of PDE sound in enclosed space.

4.3. Effective duration analysis of PDE sound in enclosed space

Hearing impairment and loudness are both related to the energy of impulse noise. When evaluating the energy of impulse noise, the effective duration and the amplitude of sound pressure are equally important. Thus, the duration becomes another important physical characteristic. Two types of durations are commonly used to assess impulse noise, *i.e.*, A duration (t_+) and B duration (t_b). The A duration is the time taken for the initial or principal pressure wave to rise to its positive peak and return momentarily to ambient pressure. The B duration is the total time taken for the envelope of the pressure fluctuations (positive and negative) to be within 20 dB of the peak pressure level.[18] Referring to the definition of impulse noise duration, the A duration and B duration of PDE sound are investigated in this research.

As shown in Fig. 10, the A and B durations of PDE sound at 20 m in enclosed space marked as t_{+1} and t_{b1} are 3.2 ms and 200 ms respectively. It can also be seen intuitively from Fig. 10 that the B duration lasts almost the whole period of PDE sound. This is because the pressure fluctuation of PDE sound in enclosed space is large after reaching the main peak pressure, and the amplitude of pressure fluctuation is within 20 dB below the peak sound pressure level.Comparing the A duration with the B duration of PDE sound at 20 m in open space, it can be seen from the figure that the t_{+2} of PDE sound in open space is determined by shock noise and jet noise, and the t_{b2} is determined by shock noise, jet noise and partial negative pressure. The t_{+2} and t_{b2} of PDE sound in open space are 1.89 ms and 5.36 ms respectively. It suggests that the values of t_+ and t_b of PDE sound in enclosed space are higher than those in open space due to the reflection and superposition of PDE sound on the walls. The ratios of t_+ to t_b in the two test environments are 1.7 and 37.3, respectively.

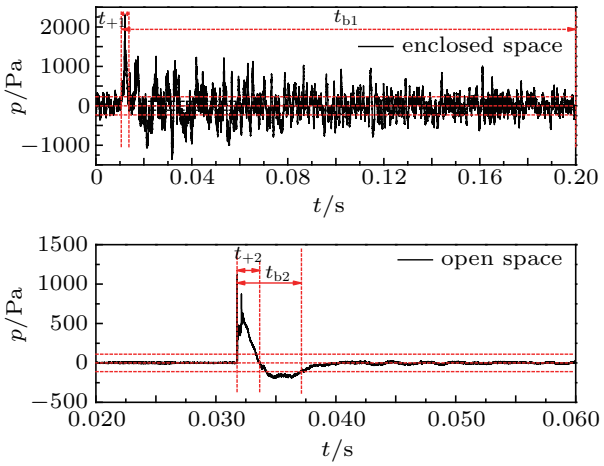


Fig. 10. Comparison between durations of PDE sound.

The values of A duration and B duration of PDE sound at different propagation distances are shown in Figs. 11(a) and 11(b). As shown in Fig. 11(a), the A duration of PDE sound in the enclosed space is generally longer than that in the open space except at the measuring points TP_{e1} and TP_{e2} which are near to the exit of PDE. As shown in Figs. 7(a) and 7(b), the reflection and superposition effects of walls on PDE sound in enclosed space are evident and the maximum sound pressure of PDE sound is the peak sound pressure of reflection noise rather than direct noise at TP_{e1} and TP_{e2}. In common with Coles,[18] the authors have found that when the measuring point is close to the sound source, the initial wave is sometimes of smaller amplitude than some of the subsequent waves, and in such a case, the A duration is taken from the largest pressure wave. As a result, the A duration of PDE sound at TP_{e1} and TP_{e2} is determined by the duration of the reflection noise. The short duration of the reflection noise results in the shorter A duration of PDE sound in the enclosed space than that in the open space.

As shown in Fig. 11(b), the B duration of PDE sound in enclosed space is significantly higher than that in open space. This is due to the higher amplitude of pressure oscillation caused by the reflection and superposition of walls on PDE sound in enclosed space, leading the B duration to increase. The decrease of shock noise, jet noise and negative pressure result in the B duration of PDE sound decreasing first and then keeping stable in open space. The B duration at the measuring point after TP_{e1} almost sustains the whole period of the PDE sound in enclosed space, indicating that the energy of reflection noise accounts for a large proportion of PDE sound.

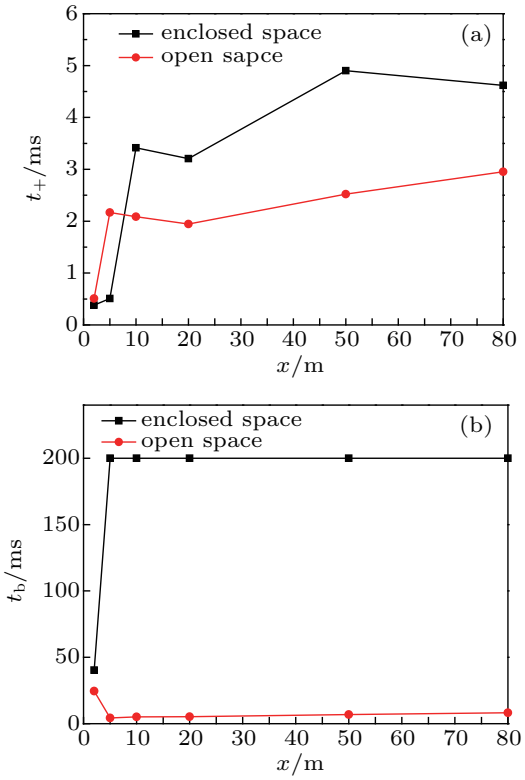


Fig. 11. Effective duration of PDE sound: (a) duration of PDE sound, (b) B duration of PDE sound.

4.4. Sound pressure level analysis of PDE sound in enclosed space

It is noticed that there are two important acoustic parameters for various types of impulse noise, *i.e.*, peak sound pressure level (PSPL) and overall sound pressure level (OASPL), the former is universally considered as the most critical factor for noise-induced hearing loss of human and defined as

$$\mathrm{PSPL} = 20\lg(P_{\mathrm{peak}}/P_0). \tag{5}$$

In formula (5), P_{peak} is the peak sound pressure of impulse noise and P_0 is the baseline sound pressure which equals 2×10^{-5} Pa.

The latter (OASPL) is defined as

$$\mathrm{OASPL} = 20\lg(P_{\mathrm{RMS}}/P_0). \tag{6}$$

In formula (6), P_{RMS} is the effective sound pressure of impulse noise and is equal to

$$P_{\mathrm{RMS}} = \sqrt{\frac{1}{T}\int_0^{\mathrm{T}} p(t)^2 \mathrm{d}t}. \tag{7}$$

The OASPL presents an amount of noise radiation energy which is also an important factor for destroying the human hearing.

Figure 12 shows the variations of PSPL of PDE sound along with propagation distance in open and enclosed space. It is found that the change rules of PSPL with the propagation distance of PDE sound in enclosed space almost coincides with that in open space. The PSPL of PDE sound generally decreases with the increase of propagation distance. In the area near the PDE exit, the PSPL of PDE sound decreases rapidly, but the attenuation rate gradually slows down with the increase of propagation distance. Comparing the PSPL of PDE sound in enclosed space with that in open space, it can be found that the PSPL of PDE sound in enclosed space is higher than those of corresponding measurement points in open space at all measuring points. The difference between the PSPL of PDE sound in enclosed space and the PSPL of PDE sound in open space at $\mathrm{TP_{e1}}$, $\mathrm{TP_{e2}}$, and $\mathrm{TP_{e3}}$ which are near the PDE exit are 3.44 dB, 2.90 dB, and 0.65 dB respectively. And the difference between the two values at $\mathrm{TP_{e4}}$, $\mathrm{TP_{e5}}$, and $\mathrm{TP_{e6}}$ which are far from the PDE exit are 6.15 dB, 18.56 dB, and 28.05 dB respectively. It suggests that the energy attenuation of PDE sound in enclosed space is much less than that in open space due to the reflection and superposition of the PDE sound on each wall. As a result, the attenuation speed of the PSPL of PDE sound in enclosed space is slower. It can also be seen from Fig. 12 that when the PDE sound propagates to the last measuring point $\mathrm{TP_{e6}}$ in enclosed space, the PSPL of PDE sound is still 159.9 dB, which indicates that the reflection and superposition of PDE sound by the solid wall of enclosed space make the PDE sound maintain high noise intensity in the far field.

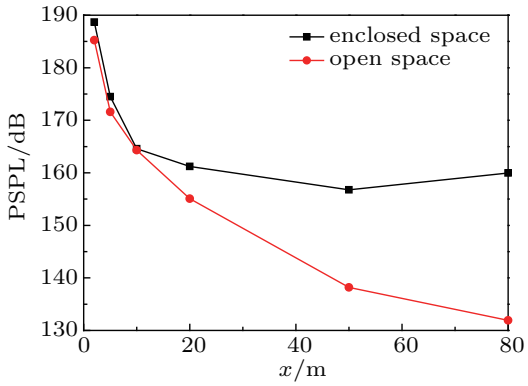


Fig. 12. Peak sound pressure level of PDE sound.

Figure 13 shows the variation of OASPL of PDE sound with propagation distance in open and enclosed space. From Fig. 13, it can be seen that the change trend and the change rules of the OASPL of PDE sound in open space and enclosed space are almost the same as those of PSPL. At the measuring point $\mathrm{TP_{e1}}$, the difference between the OASPL of PDE sound in enclosed space and that in open space is only 0.2 dB, which indicates that the energy of PDE direct noise accounts for a large proportion while the reflection noise energy accounts for a small proportion. At the measuring points after $\mathrm{TP_{e2}}$, the proportion of the reflection noise energy in the enclosed space begins to increase significantly. It is shown in the figure that the OASPL of the PDE sound in the enclosed space at the measuring point after $\mathrm{TP_{e2}}$ is much higher than that in the open space.

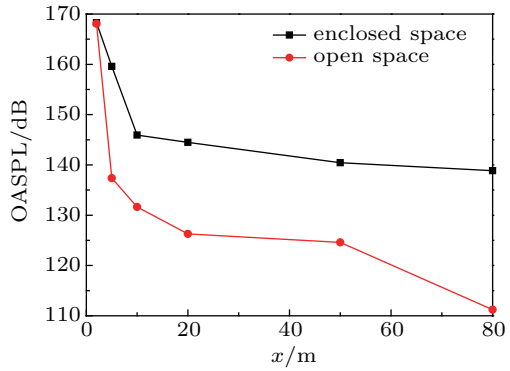


Fig. 13. Overall sound pressure level of PDE sound.

Comparing Fig. 12 with Fig. 13, it can be found that the attenuation rules of the OASPL of PDE sound is similar to that of the PSPL. The PDE sound decays rapidly near the PDE exit area and then the attenuation rate slows down, which is different from the attenuation rule of typical spherical sound wave. The attenuation amplitude and rate of PDE sound in enclosed space are much smaller than those in open space due to the reflection and superposition of PDE sound on the walls of enclosed space.

5. Conclusions

In this work, the acoustic characteristics of PDE sound propagating in enclosed space are numerically and experimentally investigated. The PDE sound is essentially produced through two sources: noise associated with shock wave and jet noise produced during the blowdown of the detonation products. The computational results clearly demonstrate the reflection and superposition process of PDE sound on the walls. The experimental results show that the acoustic characteristics of PDE sound in enclosed space are quite different from those in open space. Due to the reflection and superposition of PDE sound on the walls of enclosed space, the PDE sound waveform oscillates obviously, and in the area near the exit of PDE, the sound pressure of direct noise is less than that of reflected noise. The peak sound pressure level and overall sound pressure level of PDE sound in enclosed space are higher than those in open space. And the difference between the peak sound pressure level and overall sound pressure level of PDE sound in enclosed space increases with the rise of the propagation distance. The peak sound pressure level and overall sound pressure level of PDE sound change in the same rule that the peak sound pressure level and overall sound pressure level decrease rapidly in the area near PDE exit and the attenuation rate slows down with the increase of propagation distance. The A duration of PDE sound in enclosed space is higher than that in open space except at 2-m and 5-m measuring points. The B duration of PDE sound in enclosed space is higher than that in open space at all measuring points, and the B duration of PDE sound in enclosed space sustains the whole PDE sound period at the measuring points at the position 5 m away due to the intense pressure oscillation results from the reflection and superposition of PDE sound on the walls.

This study elaborates the acoustic characteristics of PDE sound propagating in enclosed space, which can guide the experimenters who carry out PDE experiments in the enclosed laboratory to prevent and control PDE sound. In order to avoid damaging the laboratory staffs and experimental instruments by the high intensity and long duration of PDE sound, it is suggested that the walls of the laboratory should be covered with sound-absorbing materials and the experimental equipment which are sensitive to vibration, noise and high temperature should be avoided being placed at the downstream of PDE exit. And most importantly, the experimenters are required to wear hearing protectors during the experiment.

References

[1] Kailasanath K 2003 *AIAA J.* **41** 145
[2] Boesch H E, Christian G R and Bruce T B 2000 *Army research lab Adelphi* MD No. ARL-TR-2203
[3] Allgood D, Glaser A, Caldwell N and Gutmark E 2004 *10th AIAA/CEAS AeroAcoust. Conference*, May 10, 2004, Manchester, Great Britain, p. 2879
[4] Shaw L, Harris K, Schauer F and Hoke J 2005 *11th AIAA/CEAS AeroAcoust. Conference,* May 23–25, 2005, Monterey, USA, p. 2952
[5] Glaser A, Caldwell N and Gutmark E 2006 *12th AIAA/CEAS AeroAcoust. Conference*, May 8–10, 2006, Cambridge, USA, p. 2453
[6] Glaser A, Caldwell N and Gutmark E 2007 *45th AIAA Aerosp. Sci. Meeting Exhibit*, January 8–11, 2007, Reno, USA, p. 444
[7] Caldwell N, Glaser A and Gutmark E 2007 *45th AIAA Aerosp. Sci. Meeting Exhibit*, January 8–11, 2007, Reno, USA, p. 445
[8] Zheng L X, Li N and Yan C J 2009 *47th AIAA Aerosp. Sci. Meeting Including the New Horizons Forum Aerosp. Exposition*, Janurary 5–8, 2009, Orlando, USA, p. 297
[9] Xu G Y, Weng C S, Li N and Huang X L 2016 *Int. J. Turbo. Jet Eng.* **33** 19
[10] Xu G Y, Weng C S and Li N 2014 *J. Nanjing University Sci. Technol.* **38** 781 (in Chinese)
[11] Xu G Y, Weng C S and Li N 2014 *Acta Armam.* **35** 1799 (in Chinese)
[12] Xu G Y, Weng C S, Li N and Lv X J 2015 *Acta Acoust.* **40** 579 (in Chinese)
[13] Xu G Y, Weng C S and Li N 2015 *Chin. Sciencepaper* **22** 2588 (in Chinese)
[14] Huang X L, Xu G Y, Weng C S and Li N 2015 *Acta Armam.* **36** 1855 (in Chinese)
[15] Huang X L, Weng C S, Li N and Xu G Y 2017 *J. Propul. Technol.* **38** 1194 (in Chinese)
[16] Huang X L, Weng C S, Li N and Xu G Y 2016 *Explo. Shock* **36** 633 (in Chinese)
[17] Kang Y, Li N, Weng C S and Wang C W 2018 *Chin. Phys. B* **27** 104703
[18] Coles R R A, Garinther G R and Hodge D C 1968 *J. Acoust. Soc. Am.* **43** 336